Chalcogenide Letters Vol. 10, No. 10, October 2013, p. 373 - 383

A FACILE ELECTROCHEMICAL DEPOSITION METHOD FOR NANOSTRUCTURED TELLURIDES THIN FILMS FROM CITRIC ACID BATHS

YONGBING LOU,[a,b,*] JINGJING ZHANG [a], JING LIANG [a], YAN LIU[a]
[a] *School of Chemistry and Chemical Engineering, Southeast University, Nanjing 211189, China*
[b] *Jiangsu Optoelectronic Functional Materials and Engineering Laboratory, Nanjing 211189, China*

Electrodeposition is a promising low-cost method to fabricate nanostructured thermoelectric chalcogenide thin films. However, highly acidic environment (pH $\leqslant$ 1) is always required for this kind of electrodeposition. Here we demonstrated a facile and mild electrodeposition method for binary (PbTe, Bi_2Te_3 and Sb_2Te_3) and ternary ($Bi_{0.5}Sb_{1.5}Te_3$) telluride thin films with citric acid as a complexing agent. Composition and phases of these telluride films were successfully controlled by adjusting bath composition and deposition potential. The effects of synthesis conditions on the resulting microstructure and compositional homogeneity were characterized by the X-ray diffraction pattern (XRD), field emission scanning electron microscopy (FESEM) and X-ray photoelectron spectroscopy (XPS).

(Received August 5, 2013; Accepted October 18, 2013)

Keywords: Electrodeposition, PbTe, Bi_2Te_3, Sb_2Te_3, $Bi_{0.5}Sb_{1.5}Te_3$

1. Introduction

The growing concern over increasing energy cost and global warming associated with fossil fuel sources has stimulated the search for cleaner, more sustainable energy sources. Among the viable technologies, thermoelectric (TE) energy converters have received much attention as these solid state devices can generate electricity by harvesting waste thermal energy, thereby improving the efficiency of a system. The performance of a solid state TE device is mainly determined by the magnitude of the figure-of-merit ZT ($ZT = S^2\sigma T/k$), where S is the Seebeck coefficient, σ is the electrical conductivity, k is the thermal conductivity, and T is the absolute temperature of the given TE material. All these factors are inherently correlated, thus greatly restricting the improvement of ZT.[1] Nanomaterials have been theoretically and experimentally proven to be able to partially decouple these three factors through the unique material properties at nanoscale, such as low energy electron filtering[2-4] and effective phonon scattering.[5-7]

Lead telluride (PbTe), a kind of very important narrow band gap semiconductor, is an ideal material for thermoelectric applications due to their large Bohr exciton radii (strong quantum-confinement effects) and low thermal conductivity.[8, 9] For applications at or near room temperature, tetradymite-structured materials based solid solution alloys of Bi_2Te_3, Sb_2Te_3, and Bi_2Se_3, are currently the highest performing bulk materials.[10-13] Bismuth-telluride-based alloys, such as $Bi_2Te_{2.7}Se_{0.3}$ and $Bi_{0.5}Sb_{1.5}Te_3$ forming n-type and p-type thermoelectricmaterials, are also known as the best commercially available thermoelectric materials for applications near room temperature.[14] Because of the potential for enhanced thermoelectric properties in nanoscale structures and interest in the development of thin film based devices for applications such as on-chip cooling[15-18] and thermal sensing[19]. The synthesis of high quality, crystalline thermoelectric thin films based on these materials has been actively explored.

Various methods, including ligand-based synthesis[20, 21], hydro-/solvothermal synthesis[22, 23], sonoelectrochemistry[24, 25], and chemical vapor transport[8] have been used to

* Corresponding author: lou@seu.edu.cn

produce semiconductor telluride nanostructures. However, above approaches involve complex process control, high reaction temperature, long synthesis time, and complex reagents. Electrochemical deposition has been widely used in the manufacturing of thermoelectric materials, including binary and ternary compounds due to its unique features: simple, fast, low-cost, and capable of selective deposition.[26, 27] In electrochemical depositions, the reduction and oxidation of precursor can be easily tuned by adjusting working potential. The microstructure and crystallinity of the deposited materials could be controlled by adjusting the parameters of the electrodeposition process.[28, 29] With these advantages, electrochemical deposition has been widely used in preparation of nanostructured thin film. Nanostructured PbTe, Bi_2Te_3, Sb_2Te_3 and $Bi_{0.5}Sb_{1.5}Te_3$ have been reported to be electrochemically deposited in acidic HNO_3 solution.[26, 30-45] The acidic solutions must be kept at pH $\leqslant$ 1 to dissolve enough of the cationic species. This highly acidic condition is not convenient for depositing substrates due to the highly corrosive properties of HNO_3 solution. In this paper, nanostructured PbTe, Bi_2Te_3, Sb_2Te_3 and $Bi_{0.5}Sb_{1.5}Te_3$ thin films were first electrochemically deposited by a facile procedure under a mild condition with a pH range 1.5 ~ 3.0.

2. Experimental

The cyclic voltammetry (CV) and electrodeposition experiments were carried out using a CH Instruments CHI660D electrochemical workstation connected to a three-electrode cell with a Pt disc working electrode, Pt-wire counter electrode and Ag/AgCl reference electrode at a scan rate of 100 mV/s at room temperature (25 °C). The Pb, Bi and Sb precursors were prepared by dissolving $Pb(NO_3)_2$ (Aladdin, 99.99%), $Bi(NO_3)_3$ (Sinopharm, 99.0%), and $SbCl_3$ (Sinopharm, 99.0%) in citric acid and/or nitrilotriacetate (NTA) (Sinopharm, 99%) aqueous solutions with appropriate pH value. The Te precursor, TeO_2 solution (Sinopharm, 99.99 %), was prepared by dissolving in 2M NaOH solution. The preparation of the PbTe, Bi_2Te_3, Sb_2Te_3 and $Bi_{0.5}Sb_{1.5}Te_3$ thin films was based on constant-potential electrochemical deposition at room temperature. The deposition substrate is a 99% pure Ti foil. The electrodes were cleaned with HCl 10%, rinsed with distilled water, then with acetone and dried in warm air prior to every experiment. The crystal structure and phase purity of the deposited thin films were examined with a Philips XPert Pro MPD X-ray diffractometer and filtered Cu Ka1 radiation. The binding energy of the prepared thin films was explored on the X-ray photoelectron spectrometer (PHI 5600 XPS system). FESEM characterizations were carried out with a Hitachi S-4800 FESEM equipped with an energy-dispersive X-ray spectrometer (EDS).

3. Results and Discussion

3.1 CV study for the reduction of TeO_2 solution under different pH

CV was used to select potential regions for film electrodeposition, and also for investigating the electrode processes. There were no faradaic processes observed on both Ti and Pt electrodes in the background electrolyte (0.4 M citric acid) by polarizing in a wide range of potentials.

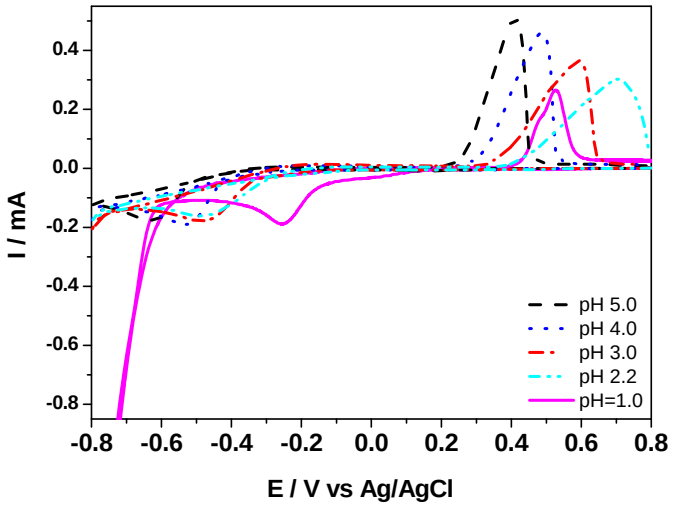

Fig. 1. CV of the solution of 0.03 M TeO_2 and 0.4 M citric acid solution at different pH values.

The TeO_2 solution is stable at pH value from 1 to 5, which provides a broad window for adjusting the reaction condition. The CV curves of TeO_2 solution at different pH value are plotted in Fig. 1. The reduction potential of TeO_2 solution shifted from −0.62 V to −0.25 V while the oxidation potential varied between 0.4 V and 0.7 V when pH value changes from 5 to 1. The reduction peak was attributed to the reduction of Te (IV) via a 4-electron process to give Te (0) [27, 46, 47]:

$$HTeO_2^+ + 3H^+ + 4\ e^- \rightarrow Te + 2H_2O \quad (1)$$

The oxidation peak corresponds to the dissolution of the deposits formed during cathodic process. It corresponds to the cathodic peak, as reported previously[47]:

$$Te + 2H_2O - 4e^- \rightarrow HTeO_2^+ + 3H^+ \quad (2)$$

With the addition of precursor cations, the mechanism of electrochemical deposition of PbTe, Bi_2Te_3, Sb_2Te_3 and $Bi_{0.5}Sb_{1.5}Te_3$ thin films has been previously proposed as [27, 46]

$$M^{n+} + n\ e^- \rightarrow M \quad (3)$$
$$m\ M + n\ Te \rightarrow M_mTe_n \quad (4)$$

Therefore, the appropriate voltage window for cations reduction and TeO_2 reduction is crucial for the electrodepostion of these tellurides. The CV study on TeO_2 revealed that the more acidic the solution is the lower reduction potential for TeO_2. This observation is consistent with previous reported reduction potential of $HTeO_3^+$ in HNO_3 solution.[38, 48, 49] The study also revealed that the electrochemical reduction of TeO_2 is preferred in acidic solution. To achieve less negative reduction potential and milder electrodeposition condition, the pH value of all the reaction solution in the following electrochemical investigation is adjusted to less than 3.

3.2 Electrochemical deposition of PbTe

The CV curves of $Pb(NO_3)_2$ solution at pH 2.1 is presented in Fig. 2a. The reduction potential of Pb^{2+} is around −0.53 V. It is similar to the reduction potential of TeO_2, which is around −0.48 V. The CV curve of the precursor mixture ($Pb(NO_3)_2$ + TeO_2) at pH 2.0 is shown in Fig. 2c, indicating a reduction peak around −0.4 V. This reduction peak could be assigned to the formation of PbTe, confirmed with an oxidation peak of PbTe found around 0.4 V. Based on these observations, the nanostructured PbTe thin film was electrochemical deposited in the precursor solution at pH 2.0, with a constant −0.4 V reduction potential vs Ag/AgCl reference electrode.

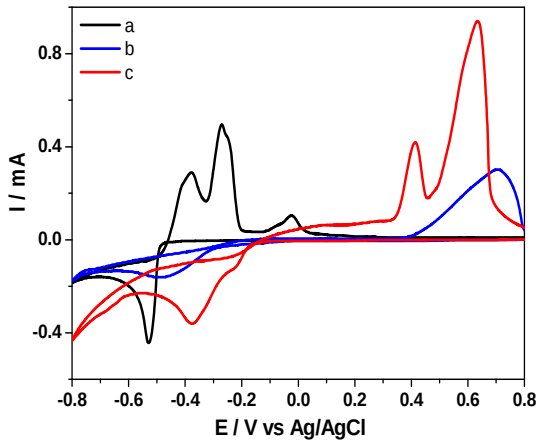

Fig. 2. CV of (a) 0.03 M $Pb(NO_3)_2$ and 0.4 M citric acid solution at pH 2.1; (b) 0.03 M TeO_2 and 0.4 M citric acid solution at pH 2.2; (c) the precursor solution of 0.03 M $Pb(NO_3)_2$, 0.03 M TeO_2 and 0.4 M citric acid solution at pH 2.0.

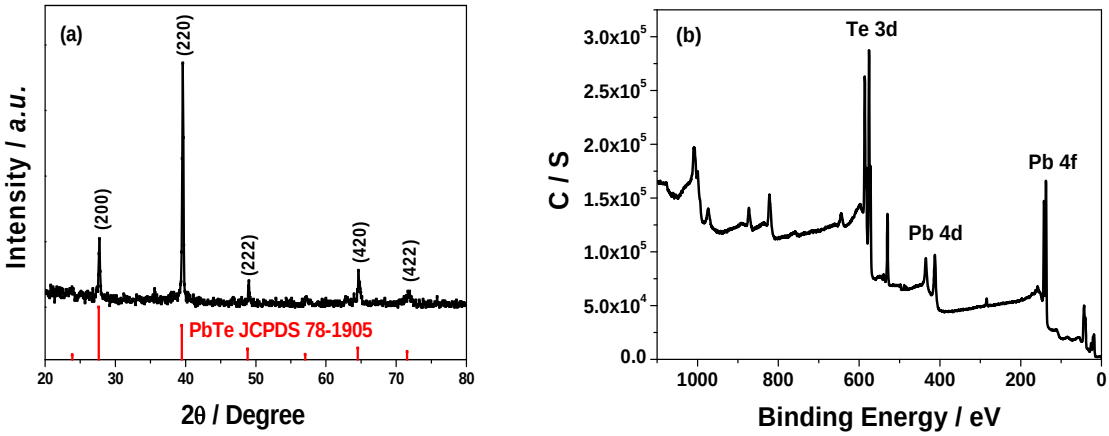

Fig. 3. (a) XRD and (b) XPS of electrochemical deposited PbTe thin film.

The XRD pattern of the electrochemically deposited thin film in Fig. 3a indicates that the deposited thin film is relatively phase pure PbTe with a polycrystalline cubic structure (JCPDS card 78-1905). The XRD pattern also indicates that the deposited PbTe thin film had a preferred crystal orientation at (2 2 0) while other researchers observed a (2 0 0) preferred crystal orientation with electrodepoistion method.[31, 50] However, there is no significant peak broadening found, which indicates the grain size of the thin film is not small enough. In order to further investigate the structure and compositions of the thin films in the present system, XPS analyses were performed for all the as-deposited films. The survey scan spectrum (Fig. 3b) of the as-deposited PbTe

thin films indicates the presence of Pb and Te in the sample. The binding energies for Pb $4f_{7/2}$ and Te $3d_{5/2}$ are 137.6 eV and 572.2 eV, respectively, which were coincided with the literature value for pure PbTe.[51]

Fig. 4a is a typical FESEM image of the surface morphology of the PbTe film. It can be seen that the PbTe film is dense and homogeneous. The film surface consists of numerous nano-particles, and the exact sizes of the nanoparticles are difficult to be determined due to agglomeration. EDS analysis gives a composition of $Pb_{0.49}Te_{0.51}$ which is close to the PbTe stoichiometry.

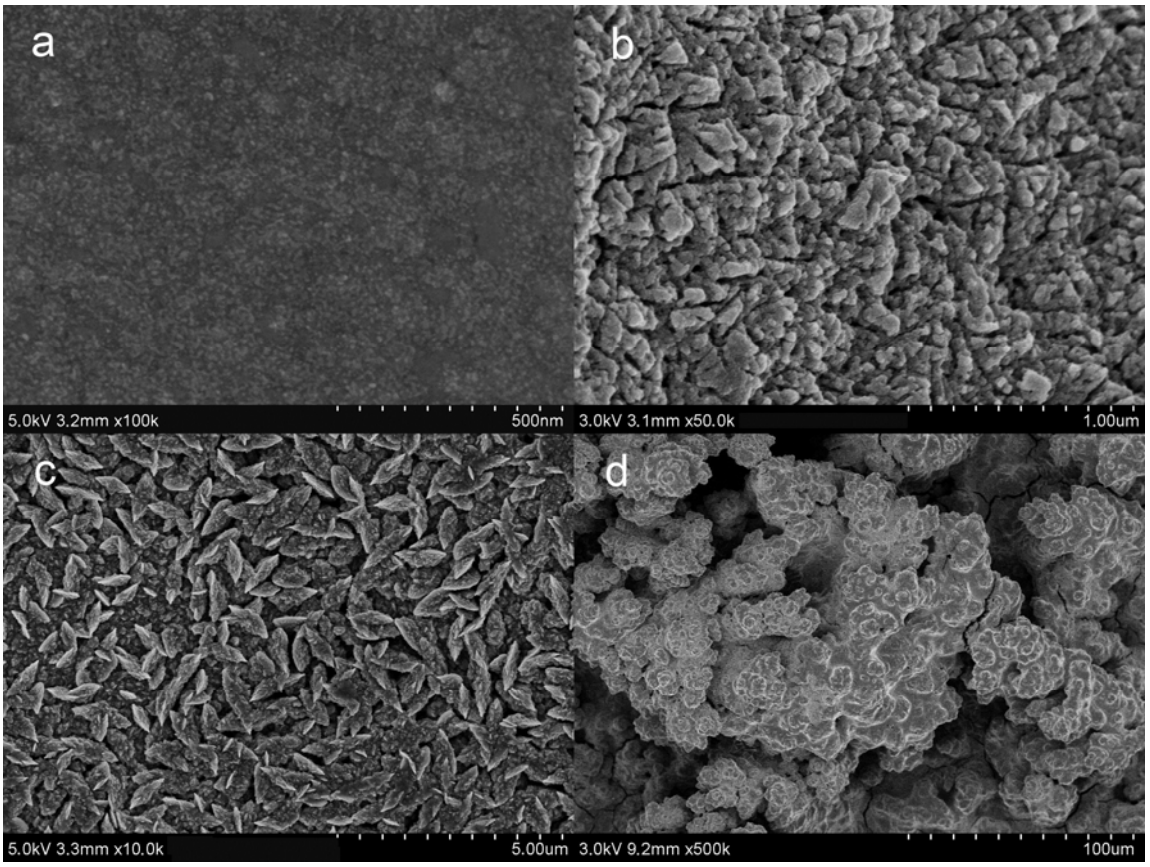

Fig. 4. FESEM images of electrochemical deposited (a) PbTe, (b) Bi_2Te_3, (c) Sb_2Te_3 and (d) $Bi_{0.5}Sb_{1.5}Te_3$ thin films.

3.3 Electrochemical Deposition of Bi_2Te_3

In the previous reports, the Bi^{3+} solution was mostly dissolved in HNO_3 solution with chelating ligand.[32, 36, 52] It was difficult to dissolve Bi^{3+} at acidic solution if it was chelated with citric acid, however, the Bi^{3+} solution could be stable when it was chelated with NTA. The CV curve of $Bi(NO_3)_3$ with NTA solution at pH 2.0 is presented in Fig. 5a. The reduction potential of Bi^{3+} is around −0.19 V. It is higher than the reduction potential of TeO_2 (ca. −0.48V) at the same pH value. The CV curve of the precursor mixture solution ($Bi(NO_3)_3$ and TeO_2) at pH 2.0 is shown in Fig. 5c. A reduction peak was found around −0.36 V, which is located between the reduction potential of TeO_2 and Bi^{3+}. This peak was ascribed to the formation of Bi_2Te_3, confirmed by a pronounced oxidation peak around 0.55 V. The small oxidation peak observed at 0.21 V is corresponding to the oxidation of bismuth-rich telluride compounds.[43] The Bi_2Te_3 thin film was electrochemical deposited in the precursor solution at pH 2.0, with a −0.5 V constant reduction potential vs Ag/AgCl reference electrode.

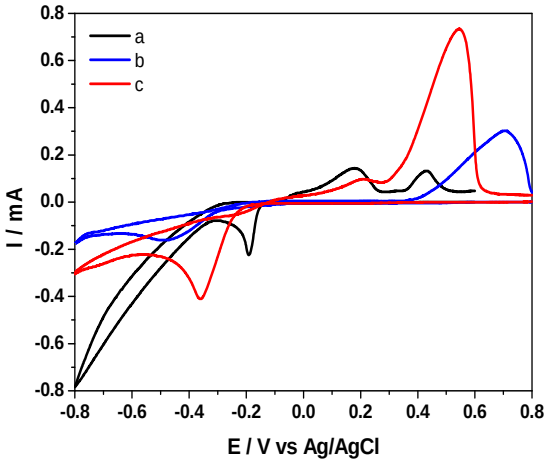

Fig. 5. CV spectra of (a) the Bi^{3+} precursor solution of 0.02 M $Bi(NO_3)_3$, 0.1 M NTA and 0.4 M citric acid solution at pH 2.0; (b) 0.03 M TeO_2 and 0.4 M citric acid solution at pH 2.2; (c) the precursor solution of 0.02 M $Bi(NO_3)_3$, 0.03 M TeO_2, 0.1 M NTA and 0.4 M citric acid solution at pH 2.0.

The XRD pattern (Fig. 6a)of the deposited thin film is consistent with standard Bi_2Te_3 data (JCPDS card 72-2036) with a polycrystalline rhombohedral structure as shown in Fig. 6a, and the peak broadening indicates the nanostructured grain size of the prepared thin film. However, the deposited Bi_2Te_3 thin film was found peel off from the Ti substrate easily. The XRD impurity peaks related to the Ti substrate confirmed the lower mechanic properties of the deposited Bi_2Te_3 thin film. The XPS survey scan spectrum (Fig. 6b) of the as-deposited Bi_2Te_3 thin films indicates the presence of Bi and Te in the sample. The Bi spectra contain one set of doublets, at binding energies of 157.3 and 162.6 eV, corresponding to the Bi $4f_{7/2}$ and Bi $4f_{5/2}$ core levels. The Te spectra also contain two sets of doublets, one with binding energies of 571.2 and 581.4 eV and the other with binding energies of 574.6 and 585.1eV, corresponding to the Te $3d_{5/2}$ and Te $3d_{3/2}$ core levels of two chemically different states.[53] The peaks at about 574.6 and 585.1 eV in the Te 3d region indicates the existence of oxidized states of Te atom on the oxidized surface while there are no oxidation states for Bi atoms on the thin film surface.

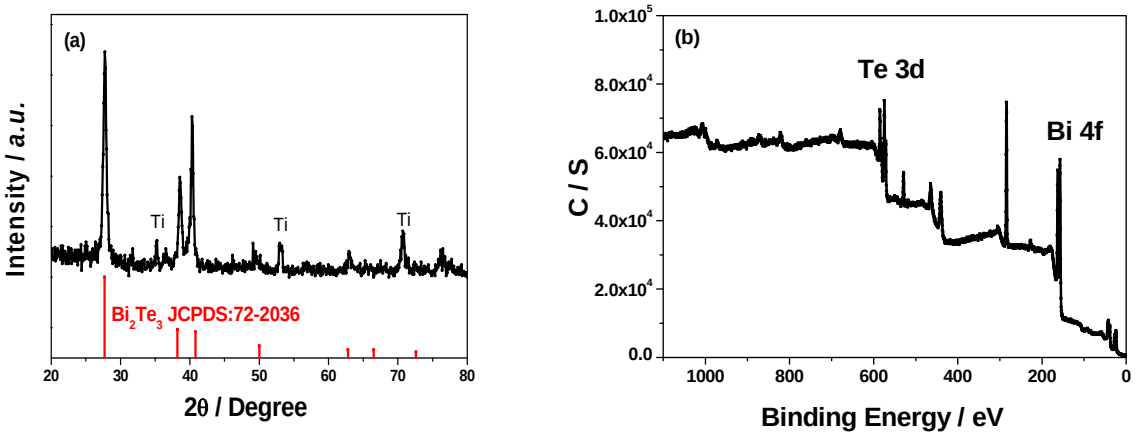

Fig. 6. (a) XRD and (b) XPS of electrochemical deposited Bi_2Te_3 thin film.

The FESEM images of as deposited Bi_2Te_3 thin film is shown in Fig. 4b. The film is very compact and relatively uniform with an average size between 50 to 200nm. The structure is similar to the solution synthesized Bi_2Te_3 nanocrystals,[54] which indicates a polycrystalline and dense

microstructure. Quantitative analysis of EDS spectrum reveals that the atomic ratio of Bi to Te is 2:3 with compositional homogeneity.

3.4 Electrochemical Deposition of Sb_2Te_3

The solution of Sb^{3+} chelated with citric acid is stable when pH < 2, which is similar to Bi^{3+}. The CV curves of $SbCl_3$ solution at pH 1.8 is presented in Fig. 7a. It can be seen that the reduction potential peak of Sb^{3+} appears at a more negative potential than that of Te, around −0.70 V. The CV curves of the precursor solution ($SbCl_3$ + TeO_2) solution at pH 1.5 is also presented in Fig. 7c. The reduction potential corresponding to the formation of Sb_2Te_3 was found at −0.24 V which was confirmed by the oxidation peak found around 0.51 V.[43] There exists another shoulder reduction peak at −0.39 V which corresponds to the TeO_2 and Sb^{3+} reduction while the oxidation peak at 0.12 V is the oxidation peak for Sb. The Sb_2Te_3 thin film was electrochemically deposited in the precursor solution at pH 1.5, under a constant −0.35V reduction potential vs Ag/AgCl reference electrode to avoid individual deposition of Sb and Te.

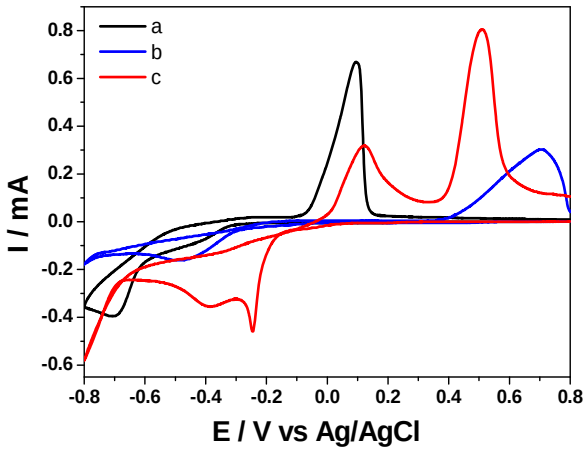

Fig. 7. CV spectra of (a) the Sb^{3+} precursor solution of 0.02 M $SbCl_3$ and 0.4 M citric acid solution at pH 1.8 ; (b) 0.03 M TeO_2 and 0.4 M citric acid solution at pH 2.2; (c) the precursor solution of 0.02 M $SbCl_3$, 0.03 M TeO_2 and 0.4 M citric acid solution at pH 1.5.

The deposited thin film is found to be amorphous based on the XRD characterization. The thin film was then annealed at 250 °C for 30 minutes. As shown in Fig. 8a, the annealed thin films show a XRD pattern, consistent with standard Sb_2Te_3 data (JCPDS card 71-0393) with a polycrystalline rhombohedral structure. This result indicates that it is hard to get crystallized Sb_2Te_3 thin film by the regular electrochemical deposition. The survey scan spectrum (Fig. 8b) of the as-deposited Sb_2Te_3 thin films indicates the presence of Sb and Te in the sample. Te $3d_{5/2}$ (572.1 eV) and Te $3d_{3/2}$ (582.5 eV) peaks are observed, while the Sb $3d_{5/2}$ and $3d_{3/2}$ peaks are observed at 529.2 and 538.5 eV, respectively, which agrees well with the results reported for Sb_2Te_3 in the literature.[55]

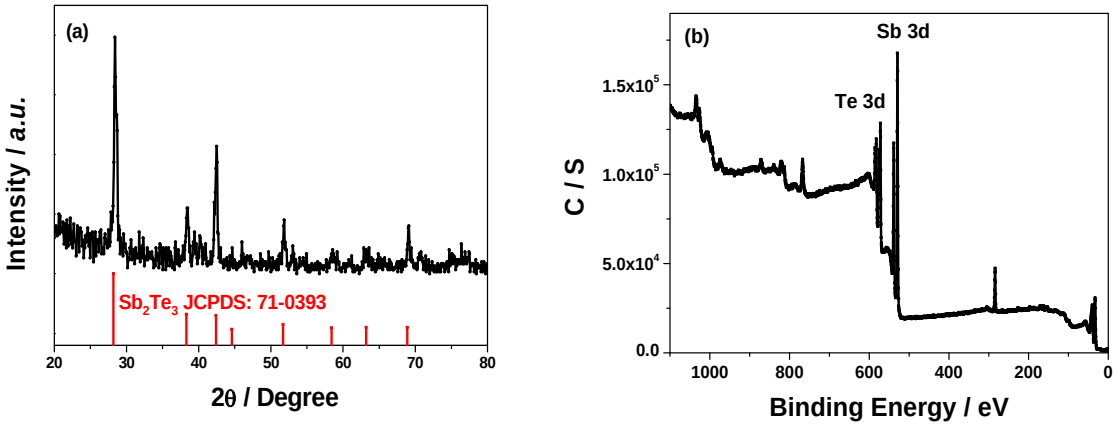

Fig. 8. (a) XRD and (b) XPS of 250 °C annealed Sb_2Te_3 thin film prepared by electrochemical deposition.

The obtained Sb_2Te_3 thin film was uniform and compact as shown in Fig. 4c. It showed a needle-like structure, which is common for Sb_2Te_3 crystal.[56] The length of Sb_2Te_3 crystal is around 1μm while the width is around 200 nm. EDS analysis indicates that the atomic ratio of Sb/Te is very close to 2:3, which further confirms that the electrodeposited film is Sb_2Te_3.

3.5 Electrochemical Deposition of $Bi_{0.5}Sb_{1.5}Te_3$

The $Bi_{0.5}Sb_{1.5}Te_3$ is the alloy of Bi_2Te_3 and Sb_2Te_3. A precursor solution of $Bi(NO_3)_3$, $SbCl_3$, citric acid, NTA and TeO_2 was prepared for electrochemical deposition based on the electrolyte bath of electrochemical depositing Bi_2Te_3 and Sb_2Te_3. The CV curves of the precursor solution at different pH value are presented in Fig. 9. The CV curves indicated the complication in electrochemical deposition of the $Bi_{0.5}Sb_{1.5}Te_3$ alloy. The CV curves revealed two cathodic peaks at potentials of −0.25 and −0.50 V, which were attributed to electrodeposition of Sb_2Te_3 and Bi_2Te_3, respectively, which were further confirmed by corresponding anodic peaks at ca 0 V, 1.8 V and 0.5 V. In the electrochemical deposition, different reduction potential was tried and it was found that different compounds formed under the different condition, and the formation of Bi_2Te_3 needed lower reduction potential than Sb_2Te_3. The $Bi_{0.5}Sb_{1.5}Te_3$ thin film was electrochemically deposited in the precursor solution at pH 3.0, with a constant reduction potential of −0.6V vs Ag/AgCl reference electrode.

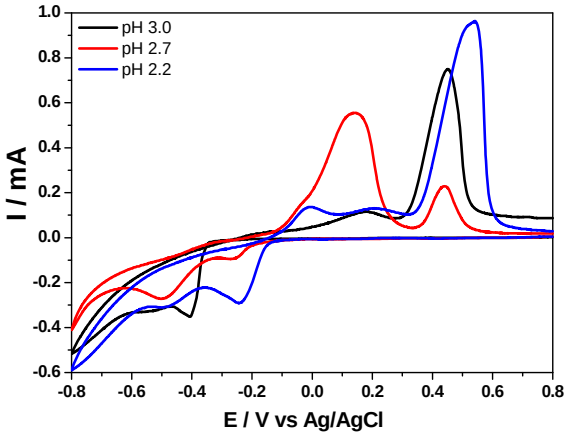

Fig. 9. Cyclic voltammogram of the precursor solution of 0.01 M $Bi(NO_3)_3$, 0.03 $SbCl_3$, 0.06 M TeO_2, 0.1 M NTA and 0.4 M citric acid solution at pH 2.2, 2.7 and 3.0.

The resulting thin films were also found to be amorphous without annealing which is similar to Sb_2Te_3. The XRD pattern (Fig. 10a) of 300 °C annealed thin film shows a XRD pattern of $Bi_{0.5}Sb_{1.5}Te_3$ with a polycrystalline rhombohedral structure (JCPDS card 49-1713). The survey scan spectrum (Fig. 10b) of the annealed $Bi_{0.5}Sb_{1.5}Te_3$ thin films indicates the presence of Bi, Sb and Te in the sample. Te $3d_{5/2}$ and Te $3d_{3/2}$ peaks are observed at (572.1 eV) and (582.5 eV). The Sb $3d_{5/2}$ and $3d_{3/2}$ peaks are observed at 529.8 and 539.0 eV. The Bi $4f_{7/2}$ and Bi $4f_{5/2}$ peaks are observed at binding energies of 157.7 and 163.2 eV. These values agreed well with the results reported for $Bi_{0.5}Sb_{1.5}Te_3$ in the literature.[57]

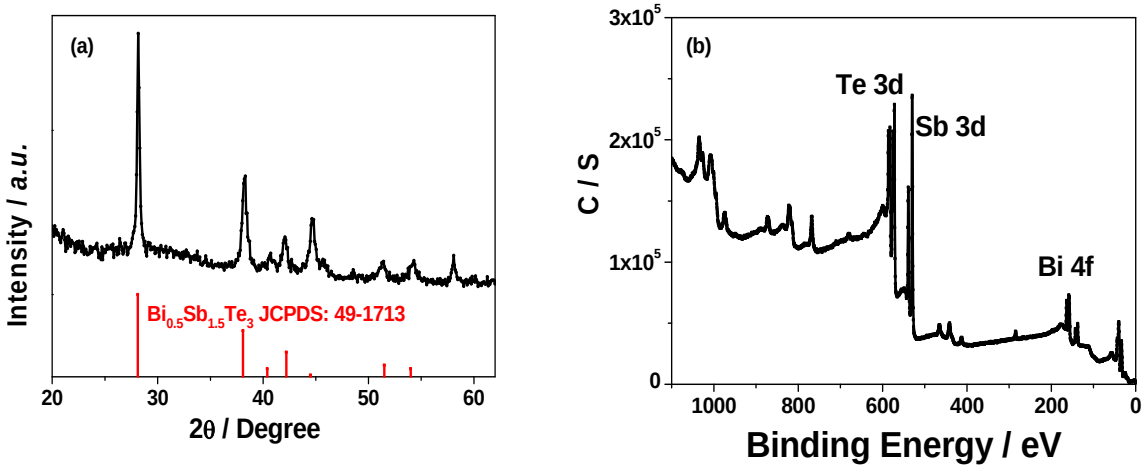

Fig. 10. (a) XRD and (b) XPS of 300 °C annealed $Bi_{0.5}Sb_{1.5}Te_3$ thin film prepared by electrochemical deposition.

The morphology of $Bi_{0.5}Sb_{1.5}Te_3$ thin film was characterized by FESEM, which indicated a cauliflower-like structure as shown in Fig. 4d. Cracks can be seen for $Bi_{0.5}Sb_{1.5}Te_3$ thin film. Post annealing is necessary for electrodeposited $Bi_{0.5}Sb_{1.5}Te_3$ thin film. The elemental composition (Bi/Sb/Te) of electrodeposited $Bi_{0.5}Sb_{1.5}Te_3$ was confirmed by EDS, which gave a mole ratio of 1/2.98/6.03.

4. Conclusion

Here we have demonstrated electrodeposition of nanostructured polycrystalline PbTe, Bi_2Te_3, Sb_2Te_3 and $Bi_{0.5}Sb_{1.5}Te_3$ thin films under a mild reaction condition through the optimization of reduction potential and the pH control of the reaction solution at room temperature. Citric acid was used as a complexing agent for all the electrodeposition precursors. NTA was added as a complexing agent to help dissolving of Bi^{3+} additionally. A pH range of 1.5 – 3.0 was used for the electrodeposition for these tellurides. The XRD analyses demonstrate that PbTe thin film on Ti substrate is of a polycrystalline structure with a dominant (2 2 0) orientation. The as-prepared Sb_2Te_3 and $Bi_{0.5}Sb_{1.5}Te_3$ films were amorphous, whereas the annealed films both had the rhombohedral structures. Surface oxidation of Te atom has been found for the as deposited thin films, which was also common in the literature report. The successful electrochemical deposition of PbTe, Bi_2Te_3, Sb_2Te_3 and $Bi_{0.5}Sb_{1.5}Te_3$ thin films indicates that electrochemical deposition is a potential choice for preparation of telluride type thermoelectric materials.

Acknowledgements

Financial support from the National Science Foundation of Jiangsu Province (No. BK2009262) and the Scientific Research Foundation for the Returned Overseas Chinese Scholars, State Education Ministry is gratefully acknowledged.

References

[1] G.J. Snyder, E.S. Toberer, Nat. Mater., **7**, 105 (2008).
[2] S.V. Faleev, F. Leonard, Phys. Rev. B, **77**, 214304 (2008).
[3] M. Zebarjadi, K. Esfarjani, A. Shakouri, J.H. Bahk, Z. Bian, G. Zeng, J. Bowers, H. Lu, J. Zide, A. Gossard, Appl. Phys. Lett., **94**, 202105 (2009).
[4] D.K. Ko, Y.J. Kang, C.B. Murry, Nano Lett., **11**,2841 (2011).
[5] K. Biswas, J. He, I.D. Blum, C.I. Wu, T.P. Hogan, D.N. Seidman, V.P. Dravid, M.G. Kanatzidis, Nature, **489**(7416), 414 (2012).
[6] S.J. Poon, K. Limtragool, J. Appl. Phys., **110**, 114306 (2011).
[7] D.G. Cahill, W.K. Ford, K.E. Goodson, G.D. Mahan, A. Majumdar, H.J. Maris, R. Merlin, S.R. Phillpot, J. Appl. Phys., **93,** 793 (2003).
[8] M. Fardy, A.I. Hochbaum, J. Goldberger, M.M. Zhang, P.D. Yang, Adv. Mater., **19**, 3047 (2007).
[9] A.L. Rogach, A. Eychmuller, S.G. Hickey, S.V. Kershaw, Small, **3**, 536 (2007).
[10] H. Scherrer, S. Scherrer, CRC Handbook of Thermoelectrics, CRC Press, 1995.
[11] D.M. Rowe, C.M. Bhandari, Modern Thermoelectrics, Holt, Rinehart and Winston, 1983.
[12] H. Zou, D.M. Rowe, S.G.K. Williams, Thin Solid Films, **408**(270 (2002).
[13] R. Venkatasubramanian, E. Siivola, T. Colpitts, B.O. Quinn, Nature, **413**(597 (2001).
[14] G.S. Nolas, J. Sharp, H.J. Goldsmid, Thermoelectrics: Basic Principles and New Materials Developments, Springer, New York, 2001.
[15] G.J. Snyder, J.R. Lim, C.-K. Huang, J.P. Fleurial, Nat. Mater., **2**(528 (2003).
[16] I. Chowdhury, R. Prasher, K. Lofgreen, G. Chrysler, S. Narasimhan, R. Mahajan, D. Koester, R. Alley, R. Venkatasubramanian, Nat. Nanotechnol., **4**,235 (2009).
[17] L.M. Goncalves, J.G. Rocha, C. Couto, P. Alpulim, J.H. Correia, Sens. Actuators A, **145**, 75 (2008).
[18] A. Shakouri, Y. Zhang, IEEE T. Compon. Pack. T., **28**(65 (2005).
[19] A. Boyer, E. Cisse, Mater. Sci. Eng. B, **13**(103 (1992).
[20] Y. Pan, H. Bai, L. Pan, Y. Li, M.C. Tamargo, M. Sohel, J.R. Lombardi, J. Mater. Chem., **22**(44):23593-23601 (2012).
[21] Y. Zhao, J.S. Dyck, C. Burda, J. Mater. Chem., **21**(43):17049-17058 (2011).
[22] G. Tai, B. Zhou, W. Guo, J. Phys. Chem. C, **112**(11314): (2008).
[23] L. Kungumadevi, R. Sathyamoorthy, Adv. Powder Technol., **24**(1):218-223 (2013).
[24] X.F. Qiu, Y.B. Lou, A.C.S. Samia, A. Devadoss, J.D. Burgess, S. Dayal, C. Burda, Angew. Chem. Int. Ed., **44**(5855-5857 (2005).
[25] B. Qiu, Y. Ni, L. Zhang, J. Cryst. Growth, **310**(4199 (2008).
[26] W. Glatz, L. Durrer, E. Schwyter, C. Hierold, Electrochim. Acta, **54**(2):755-762 (2008).
[27] F. Xiao, C. Hangarter, B. Yoo, Y. Rheem, K.-H. Lee, N.V. Myung, Electrochim. Acta, **53**(28):8103-8117 (2008).
[28] C.X. Xiang, Y.G. Yang, R.M. Penner, Chem. Commun., **859-873.**((2009).
[29] W.F. Liu, W.L. Cai, L.Z. Yao, Chem. Lett., **36**(1362-1363 (2007).
[30] K. Chatterjee, A. Suresh, S. Ganguly, K. Kargupta, D. Banerjee, Mater. Charact., **60**(12):1597-1601 (2009).
[31] I.Y. Erdogan, T. Oznuluer, F. Bulbul, U. Demir, Thin Solid Films, **517**(5419-5424 (2009).
[32] P. Heo, K. Hagiwara, R. Ichino, M. Okido, J. Electrochem. Soc., **153**(213-217 (2006).
[33] H. Kose, M. Bicer, C. Tutunoglu, A.O. Aydin, I. Sisman, Electrochim. Acta, **54**(1680-1686 (2009).
[34] F.H. Li, Q.H. Huang, W. Wang, Electrochim. Acta, **54**(3745-3752 (2009).
[35] F.H. Li, W. Wang, Appl. Surf. Sci., **255**(4225-4231 (2009).
[36] G.R. Li, F.L. Zheng, Y.X. Tong, Cryst. Growth Des., **8**(1226-1232 (2008).
[37] A. Mondal, N. Mukherjee, S.K. Bhar, D.B. Ee, Thin Solid Films, **515**(1255-1259 (2006).
[38] H. Saloniemi, M. Kemell, P. Ritala, M. Leskela, J. Electroanal. Chem., **482**(139-148 (2000).
[39] W. Zhu, J.Y. Yang, D.X. Zhou, C.J. Xiao, X.K. Duan, Langmuir, **24**(5919 (2008).

[40] Y. Ma, E. Ahlberg, Y. Sun, B.B. Iversen, A.E.C. Palmqvist, Electrochim. Acta, **56**(11):4216-4223 (2011).
[41] H. Jung, N.V. Myung, Electrochim. Acta, **56**(16):5611-5615 (2011).
[42] I.-J. Yoo, Y. Song, D. Chan Lim, N.V. Myung, K.H. Lee, M. Oh, D. Lee, Y.D. Kim, S. Kim, Y.-H. Choa, J.Y. Lee, K.H. Lee, J.-H. Lim, J. Mater. Chem. A, **1**(17):5430-5435 (2013).
[43] Y. Ma, E. Ahlberg, Y. Sun, B.B. Iversen, A.E.C. Palmqvist, J. Electrochem. Soc., **159**(2):D50-D58 (2012).
[44] M. Bicer, I. Sisman, Langmuir, **28**(44):15736-15742 (2012).
[45] H.P. Nguyen, X. Peng, G. Murugan, R.J.M. Vullers, P.M. Vereecken, J. Fransaer, J. Electrochem. Soc., **160**(2):D75-D79 (2012).
[46] D.W. Liu, J.F. Li, J. Electrochem. Soc., **155**(493-498 (2008).
[47] E. Mori, C.K. Baker, J.R. Reynolds, K. Rajeshwar, J. Electroanal. Chem., **252**(441 (1988).
[48] F. Golgovici, A. Cojocaru, M. Nedelcu, T. Visan, Chalcogenide Lett., **6**(323-333 (2009).
[49] Y.A. Ivanova, D.K. Ivanou, E.A. Streltsov, Electrochim. Acta, **52**(5213-5218 (2007).
[50] H. Saloniemi, T. Kanniainen, M. Ritala, M. Leskelä, Thin Solid Films, **326**(1-2):78-82 (1998).
[51] M. Bettini, H.J. Richter, Surf. Sci., **80**(334-343 (1979).
[52] S. Li, H.M.A. Soliman, J. Zhou, M.S. Toprak, M. Muhammed, D. Platzek, P. Ziolkowski, E. Müller, Chem. Mater., **20**(13):4403-4410 (2008).
[53] J. Fu, S. Song, X. Zhang, F. Cao, L. Zhou, X. Li, H. Zhang, CrystEngComm, **14**(6):2159-2165 (2012).
[54] Y. Zhao, J.S. Dyck, B.M. Hernandez, C. Burda, J. Phys. Chem. C, **114**(26):11607-11613 (2010).
[55] S.S. Garje, D.J. Eisler, J.S. Ritch, M. Afzaal, P. O'Brien, T. Chivers, J. Am. Chem. Soc., **128**(10):3120-3121 (2006).
[56] G. Leimkühler, I. Kerkamm, R. Reineke-Koch, J. Electrochem. Soc., **149**(10):C474-C478 (2002).
[57] Y. Zhao, C. Burda, ACS Appl. Mater. Inter., **1**(6):1259-1263 (2009).